# On the Link Modeling of Static Wireless Sensor Networks in Ocean Environments

Alireza Shahanaghi, Yaling Yang, and R. Michael Buehrer
Department of Electrical and Computer Engineering, Virginia Tech
Email: {shahan,yyang8,buehrer}@vt.edu

***Abstract*—Despite of the advantages that ocean surface Wireless Sensor Networks (WSN) have over traditional ocean monitoring methods, ocean WSN research suffers from lack of an accurate model that describes the stability of wireless links among sensor nodes. In this paper, we are going to investigate ocean surface waves' effects on the Line-of-Sight (LoS) link between sensors in a homogeneous WSN. Specifically, we will derive the blocking probability of LoS links between a transmitter and receiver pair due to wave movements, and analyze how environmental effects like wind speed affects it. Simulation results along with oceanographic measurements validates our analyses, making our model applicable in design and planning of WSN in ocean environment.**

***Index Terms*—Wireless Sensor Network, marine communications, Line-Of-Sight link stability, maximum wave-height, link stability**

## I. Introduction

Comparing to conventional marine research vessels, ocean surface wireless sensor networks (WSN) have many advantages for ocean monitoring studies, including dramatic improvement in access to real-time data for long periods of time, larger geographical coverage of ocean areas, higher resolution monitoring of marine environments, more rapid processing of collected data and instantaneous transmission of data to monitoring centers in the shore [1]. Consisting of sensor nodes with simple structures, ocean WSN can decrease the cost by at least one order of magnitude comparing to marine research vessel approach [2].

Despite of the advantages of ocean WSN, ocean WSN research suffers from lack of an accurate model that describes the wireless links among sensor nodes [3]–[5]. While some existing literatures have proposed accurate models of the radio-wave propagation and reflection over ocean surface [6], these models assume either one or both transmitter and receiver antennas are much higher than the ocean surface level, e.g., a vessel and an onshore base station. However, the heights of antennas of most sensors in ocean WSN are short. When the weather is rough, the height of ocean waves can exceed the antenna height. Since electromagnetic waves cannot penetrate salt water, occurrence of waves higher than antenna height blocks the Line-of-Sight (LoS) link between the transmit sensor and the receiver, causing disruption to wireless communications. Unfortunately, existing literatures have not taken into account of this kind of disruptions to wireless links. Without proper link-stability understanding, network protocols designed for ocean WSN are not robust to disruptions in bad weather, which results in decreasing network reliability [4].

To fill in this void, in this paper, we are going to present a model that captures the effects of wave-height on the line-of-sight (LoS) link between the transmitter and receiver. Then, using the model, we will obtain the blocking probability of LoS link and verify that with simulation results. Our work is the first that provides a realistic and tractable model of link stability under different weather conditions in ocean WSN. This result can provide important guidelines for network protocol designs in ocean WSN.

Building an accurate model to describe ocean waves' impact on LoS wireless link is a non-trivial task. The very few research papers in the area of ocean WSN that does not ignore the probability of link blocking due to wave-height use an over-simplified ocean model [7] . They assume ocean surface fluctuates according to a single sine wave and ignore environmental parameters like wind speed which have an important effects on ocean surface displacement. Real ocean waves are much more complicated than a sine wave, making these papers' results unrealistic.

While statistical models that accurately describe the ocean surface behavior are available in oceanographic research, all of these models focus only on temporal behavior of ocean waves. Such temporal behavior models are useful in traditional ocean and coastal engineering, which only needs to consider the temporal characteristics of ocean surface at a specific site. However, in ocean WSN, the quality of a wireless link depends on the states of the entire ocean surface area between the transmitter and receiver, which can span many kilometers. Describing the LoS wireless links for the ocean WSN, thus, requires a tractable model of ocean surface in spatial domain, which is lacking in existing literatures.

To further complicate the situation, existing oceanographic works focus on deriving statistics that are useful in ocean engineering fields. Many statistics that are significant for communication systems cannot be found in oceanographic studies. For example, in order to understand statistical similarities between different parts of a wireless link, spatial autocorrelation function behavior should be determined; however, oceanographic works mostly do not focus on auto-correlation function and efforts in specific cases like [8]–[10] results in intractable integrals and complicated functions.

In this paper, we address the challenges and build a tractable and accurate model for LoS link in ocean WSN through

the following steps. First, we obtain the average wave-length and derive a simple model for describing the spatial auto-correlation behavior based on existing oceanographic models. Using the model of auto-correlation, we define the coherence distance and divide the waves between transmitter and receiver into semi-independent profiles using the coherence distance. Then, we derive the Probability Density Function (PDF) of local maximum wave-height of each profile. Next, using the derived local maximum PDF and concept of semi-independent wave profiles, we obtain the PDF of global maximum wave-height occurring between transmitter and receiver. Finally using the PDF of global maximum wave-height, we obtain the probability of LoS blocking and validate that with simulation results.

The rest of this paper is organized as follows. In Section II we will have a brief review about ocean wave modeling and spectra that are widely accepted in oceanographic studies and used in ocean and coastal engineering. In Section III, we will discuss spatial autocorrelation function, and approximate its envelope with respect to the average wavelength. Using the approximated envelope of spatial autocorrelation, we will obtain the PDF of local and global maximum wave-height in Section IV and use that for calculating the blocking probability of LoS link between a transmitter and receiver pair in a homogeneous WSN. Finally, in Section V, we will evaluate our mathematical analysis regarding LoS link blocking and validate them by simulation results.

## II. Ocean Wave Modeling

In this section, we are going to have a brief review about linear wave theory, which is the foundation for our analysis of wireless link stability. Linear wave theory is an ocean wave model that has been widely used in ocean and coastal engineering and has been shown to perfectly match with the spectral description of real ocean waves in deep water, where the wave amplitude is small comparing to the wavelength and water depth. [11], [12] Specifically, linear wave theory models the ocean surface displacement as a linear summation of large number of harmonic waves, each of which is propagated independently without any effect on the others. Denoting $\xi(\underline{\mathbf{x}}, t)$ as the ocean surface displacement in Cartesian coordination of $\underline{\mathbf{x}} = (x, y)$ and time $t$, linear wave theory claims

$$\xi(\underline{\mathbf{x}}, t) = \sum_{\underline{\boldsymbol{\kappa}}} a(\underline{\boldsymbol{\kappa}}) \cos\big(\underline{\boldsymbol{\kappa}} \cdot \underline{\mathbf{x}} - \omega t + \theta(\underline{\boldsymbol{\kappa}})\big), \tag{1}$$

where $\underline{\boldsymbol{\kappa}} = (\kappa_1, \kappa_2)$ is called wave-vector. Constants $a(\underline{\boldsymbol{\kappa}})$ and $\theta(\underline{\boldsymbol{\kappa}})$ are independent random variables corresponding to amplitudes and phases of harmonic waves respectively. $\omega$ is the angular frequency, which relates to its corresponding wave-vector by dispersion equation

$$\omega^2 = g\boldsymbol{\kappa} \tanh(\boldsymbol{\kappa} D), \tag{2}$$

where $D$ represents the depth of ocean water, $g \approx 9.807 m/s^2$ is the standard acceleration of gravity , and $\boldsymbol{\kappa} = \sqrt{\kappa_1^2 + \kappa_2^2}$ is the Frobenius norm of $\underline{\boldsymbol{\kappa}}$. For the case of deep water waves, which is the focus of this paper, we have $\boldsymbol{\kappa} D \gg 1$ and the dispersion equation (2) can be simplified to $\omega^2 = g\boldsymbol{\kappa}$.

Theoretical analysis using central limit theorem as well as statistical analysis of data sets obtained from wave-buoys and remote sensing measurements have all revealed that $\xi(\underline{\mathbf{x}}, t)$ is a wide sense stationary (WSS) Gaussian random process of mean 0 [13]. For WSS processes, the total power $P$ can be obtained by integration of power spectral density. Applying change of variables and dispersion equation on this integration for ocean waves, the total power is given by [11], [12] as :

$$P = \int_{\omega=0}^{\infty} \int_{\vartheta=-\pi}^{\pi} E(\omega, \vartheta) \mathrm{d}\omega \mathrm{d}\vartheta. \tag{3}$$

$E(\omega, \vartheta)$ is called the ocean waves' directional spectrum which represents the distribution of ocean wave energy in frequency $\omega$ and direction $\vartheta$. Oceanographic investigations [11], [14] have revealed that $E(\omega, \vartheta)$ can be factorized as $E(\omega, \vartheta) = S(\omega)\Omega(\vartheta)$ such that $\int_{-\pi}^{\pi} \Omega(\vartheta) \mathrm{d}\vartheta = 1$. $\Omega(\vartheta)$ is called directional distribution and $S(\omega)$ is called ocean wave spectrum. Setting the Cartesian coordinate system such that the x-axis is along the wind direction, $\Omega(\vartheta)$ is an even function defined over $-\pi \leq \vartheta < \pi$ with a maximum at $\vartheta = 0$. $S(\omega)$ is a single-sided function defined on $0 \leq \omega < \infty$. The exact forms of $\Omega(\vartheta)$ and $S(\omega)$ differ among different ocean wave models. The expression of $S(\omega)$ is related to wind speed, and $\Omega(\vartheta)$ is determined by wind direction. For detailed information on different directional distributions and wave spectra, readers can refer to [14] and [15].

## III. Spatial Autocorrelation Function

In Section II, we had a brief review on the state-of-art model of ocean waves and spectra. As we discussed, ocean surface displacement is a WSS zero mean Gaussian process. In general, WSS Gaussian processes can be completely characterized by their mean and linear autocorrelation function. In this section, we are going to investigate the autocorrelation function in space domain, which then will be used to analyze the LoS link stability of ocean WSN in section IV.

Providing an exact closed form expression for the spatial autocorrelation function of ocean wave is not mathematically possible. To cope with this challenge, we will use an approximation approach in this section. In essence, there is no need to have the exact expression of spatial autocorrelation function for analyzing the LoS link stability. In our follow-up analysis of link stability, we will derive the envelope of the autocorrelation function and use it as the approximation of autocorrelation function.

In Section III-A, we will first identify the expression of the envelope of normalized autocorrelation function in space domain based on oceanographic measurements in time domain [11], [16]. In Section III-B, we will further show how to derive average wavelength, which is the key parameter in this envelope expression.

### A. Spatial Autocorrelation Envelope

At a given time $t$, the spatial autocorrelation function of ocean surface is defined as:

$$R_\xi(\delta_x, \delta_y, t) = \mathbb{E}\{\xi(x+\delta_x, y+\delta_y, t)\xi(x, y, t)\}, \quad (4)$$

where $\mathbb{E}\{.\}$ represents the statistical expected value. $R_\xi(\delta_x, \delta_y, t)$ describes the joint statistical behavior of two ocean surface positions whose distance is defined by vector $(\delta_x, \delta_y)$. In the remainder of this paper, for simplicity of notation, we will use $R_\xi(\delta_x, \delta_y)$ for representing the spatial autocorrelation for a given fixed $t$.

According to Wiener-Khinchin theorem [17], the autocorrelation function of a WSS random process can be obtain by inverse Fourier transform of its power spectral density. Combining Wiener-Khinchin theorem and the concept of directional spectrum, it can be shown that [8], [10] $R_\xi(\delta_x, \delta_y)$ for deep water waves can be obtained by semi-inverse cosine Fourier transform of $E(\omega, \vartheta)$ such that :

$$R_\xi(\delta_x, \delta_y) = \int_{\omega=0}^{\infty}\int_{\vartheta=-\pi}^{\pi} E(\omega, \vartheta) \times \cos\left(\frac{\omega^2}{g}[\cos(\vartheta)\delta_x + \sin(\vartheta)\delta_y]\right) \mathrm{d}\omega\mathrm{d}\vartheta. \quad (5)$$

Since we are going to use the spatial autocorrelation expression for describing the link between a transmitter and receiver, we change Cartesian distance vector of $(\delta_x, \delta_y)$ to the polar coordination $(l, \phi)$ to facilitate the expression of transmitter-receiver distance. The x-axis is directed along the wind direction (downwind) and y-axis is perpendicular to wind direction (crosswind). Without loss of generality, we assume the origin of coordinate system is set to the transmitter location. Therefore, $l$ denotes the distance between transmitter and receiver, and $\phi$ is the angle from the positive side of x-axis such that $\delta_x = l\cos(\phi)$ and $\delta_y = l\sin(\phi)$. Substituting $E(\omega, \vartheta) = S(\omega)\Omega(\vartheta)$, (5) is transformed to the following polar representation:

$$R_\xi(l, \phi) = \int_{\omega=0}^{\infty}\int_{\vartheta=-\pi}^{\pi} S(\omega)\Omega(\vartheta) \times \cos\left(\frac{\omega^2}{g} l\cos(\vartheta - \phi)\right) \mathrm{d}\omega\mathrm{d}\vartheta. \quad (6)$$

In the remainder of this paper, we assume that sensors are not moving horizontally such that the polar angle $\phi$ is fixed. Thus, we can treat $\phi$ in (6) as a constant and use $R_\xi(l)$ instead of $R_\xi(l, \phi)$ to show that the spatial autocorrelation is only a function of $l$.

In general, integrals of (6) can not be simplified to a closed-form tractable expression. Some existing efforts [8], [10] in the literature tried to simplify these integrals for specific cases of $S(\omega)$ and $\Omega(\vartheta)$. But, their results are not generally applicable for most ocean wave models. In addition, these efforts mostly resulted in some series and special functions which are too complicated for further analysis, making them not useful for deriving link stability metrics.

To deal with this challenge, we note that for link stability analysis, it is not essential to have the exact mathematical integration result from (6). Thus, in this work, we are going to approximate the envelope of spatial autocorrelation function, which is sufficient for analyzing the link behavior. This approximation method can greatly simplify the issue of link stability analysis and can also potentially facilitate similar future works. Our simulation results in Section V have shown that this approximation method produces very accurate results.

In order to approximate the autocorrelation function in space domain, we take a closer look at the general stochastic process of ocean surface displacement expression in (1). Consider (1) in polar coordination, which yields

$$\xi(l, \phi, t) = \sum_{(\kappa_1, \kappa_2)} a(\kappa_1, \kappa_2) \cos\Big([\kappa_1\cos(\phi) + \kappa_2\sin(\phi)]l - \omega t + \theta(\kappa_1, \kappa_2)\Big), \quad (7)$$

where $x = l\cos(\phi)$ and $y = l\sin(\phi)$. For a constant $\phi$, by fixing one of $l$ or $t$ in (7), $\xi(l, \phi, t)$ will turn into a one dimensional WSS zero-mean Gaussian process in time or space domain. Without loss of generality, we can set $l$ and $t$ to 0 in (7) which yields

$$\xi(l=0, \phi, t) = \sum_{(\kappa_1, \kappa_2)} a(\kappa_1, \kappa_2)\cos\left(-\omega t + \theta(\kappa_1, \kappa_2)\right) \quad (8)$$

and

$$\xi(l, \phi, t=0) = \sum_{(\kappa_1, \kappa_2)} a(\kappa_1, \kappa_2) \cos\Big([\kappa_1\cos(\phi) + \kappa_2\sin(\phi)]l + \theta(\kappa_1, \kappa_2)\Big), \quad (9)$$

as ocean surface displacement in time and space domain. As can be seen, both of (8) and (9) are generated by summation of infinite number of independent harmonic waves each of which has random amplitude and phase corresponding to the wave-vector. This similarity brings the temporal and spatial autocorrelation about to have the same behavior.

Oceanographic measurements in time domain reveal that the envelope of normalized temporal autocorrelation decays exponentially with respect to the average period of ocean waves [11], [16] in the form of

$$R_\xi^{\text{temporal}}(\tau) \propto \exp(-\tau/\overline{T}),$$

where $\tau$ is the time difference, and $\overline{T}$ is the average period of ocean waves. Based on the stochastic similarities between processes of ocean surface displacement in time and space domains shown in (8) and (9), we can model the envelope of normalized spatial auto-correlation by an exponential function of average spatial period of ocean waves as well. Fixing the polar angle in (6), we have

$$R_\xi(l) \propto \exp(-l/\overline{\lambda}), \quad (10)$$

where $\overline{\lambda}$ is the average wave length (i.e. the average spatial wave period), which we will discuss how to compute it in the next subsection.

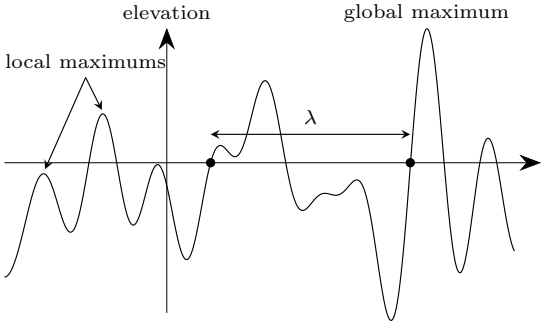


Fig. 1: A simple illustration of surface displacement in space domain

### B. Average Wavelength

To define the average wavelength of ocean waves, consider the ocean surface displacement of (9) in space domain when $\phi$ is constant. With a slight abuse of notation, we use $\xi(l)$ for demonstrating ocean surface displacement in this case. Fig. 1 depicts a simple illustration of $\xi(l)$ fluctuating around zero level since it is a zero-mean stochastic process. As can be seen, there exists two kinds of zero-crossing points in the figure; upward zero-crossing point after which the surface elevation is above the zero (mean) level, and downward zero-crossing after which the surface elevation goes beneath the zero level. Using the concept of zero-crossing, wavelength $\lambda$ can be defined as the distance between two successive upward (downward) zero-crossing points.

In order to obtain the average wavelength, we are going to derive the average number of zero-crossings first. Let $\underline{\mathbf{a}}$ be the set of all random amplitudes of harmonic waves, and $\underline{\boldsymbol{\theta}}$ be the set of all random phases in (10). $\xi(l)$ can be interpreted as a random curve which is a function of stochastic sets $\underline{\mathbf{a}}$ and $\underline{\boldsymbol{\theta}}$, and a deterministic variable $l$, i.e., $\xi(l) \equiv F(\underline{\mathbf{a}}, \underline{\boldsymbol{\theta}}; l)$. Let $\xi'(l)$ be the derivative of $\xi(l)$ with respect to $l$, i.e., $\xi'(l) = \partial F(\underline{\mathbf{a}}, \underline{\boldsymbol{\theta}}; l)/\partial l$. We define $\xi_l$ and $\xi'_l$ as samples of $\xi(l)$ and $\xi'(l)$ in a certain $l$ respectively. $\xi(l)$ is a WSS zero-mean Gaussian process which necessitates $\xi'(l)$ to be a WSS zero-mean Gaussian process. Moreover, $\xi(l)$ and $\xi'(l)$ will be jointly WSS Gaussian processes [17]. Therefore, $\xi_l$ and $\xi'_l$ are zero-mean jointly Gaussian random variables described by bivariate normal distribution function of $f(\xi_l, \xi'_l; l)$ [17]. From [18], it can be shown that the average number of zero-crossings $\overline{N}_z$ of a random curve $\xi(l)$ over a given interval $(l_1, l_2)$ can be obtained as

$$\overline{N}_z = \int_{l=l_1}^{l_2} \int_{\xi'_l=-\infty}^{\infty} |\xi'_l| f(0, \xi'_l; l) \mathrm{d}\xi'_l \mathrm{d}l. \tag{11}$$

To compute the above integration, note that $\xi_l$ and $\xi'_l$ are jointly Gaussian random variables. Hence, $f(0, \xi'_l; l)$ can be jointly described by their first order (mean) and second order (variance and correlation coefficient) statistics. As it has been mentioned before, $\xi_l$ and $\xi'_l$ are both zero mean. Next, we will show how to compute their second order statistics.

Define the $r$th moment of wave spectrum $S(\omega)$ as

$$m(r) := \int_0^{\infty} \omega^r S(\omega) \mathrm{d}\omega. \tag{12}$$

Variance of $\xi_l$ ($\sigma^2_{\xi_l}$) can be obtained by substituting $l = 0$ in (6) which yields

$$\sigma^2_{\xi_l} = \int_{\omega=0}^{\infty} \int_{\vartheta=-\pi}^{\pi} S(\omega)\Omega(\vartheta) \mathrm{d}\omega \mathrm{d}\vartheta = m(0). \tag{13}$$

In order to obtain the variance of $\xi'_l$, first note that for WSS stochastic processes, the autocorrelation function of $\xi'(l)$, which is denoted as $R_{\xi'}(l, \phi)$, can be computed as follows [17]:

$$R_{\xi'}(l, \phi) = -\frac{\partial^2}{\partial l^2} R_{\xi}(l, \phi). \tag{14}$$

Considering (6) and (12), variance of $\xi'_l$ ($\sigma^2_{\xi'_l}$) can be obtained by substituting $l = 0$ in (14), which yields

$$\begin{aligned} \sigma^2_{\xi'_l} &= \int_{\omega=0}^{\infty} \int_{\vartheta=-\pi}^{\pi} \frac{\omega^4}{g^2} S(\omega) \cos^2(\vartheta - \phi)\Omega(\vartheta) \mathrm{d}\omega \mathrm{d}\vartheta \\ &= \frac{m(4)}{g^2} \int_{-\pi}^{\pi} \cos^2(\vartheta - \phi)\Omega(\vartheta) \mathrm{d}\vartheta. \end{aligned} \tag{15}$$

In order for computing the correlation coefficient of $\xi_l$ and $\xi'_l$, the distribution of random sets $\underline{\mathbf{a}}$ and $\underline{\boldsymbol{\theta}}$ should be known. One of the typical assumptions usually made for WSS stochastic processes of form (9) is that each harmonic has a phase uniformly distributed over $[-\pi, \pi)$, which is valid for ocean waves [19]. This assumption is a sufficient condition for $\xi_l$ and $\xi'_l$ to be uncorrelated and consequently independent since both of these random variables are Gaussian. Therefore, $f(\xi_l, \xi'_l; l)$ will be equivalent to the multiplication of two normal PDFs corresponding to $\xi_l$ and $\xi'_l$, i.e.,

$$f(\xi_l, \xi'_l; l) = \frac{1}{2\pi\sigma_{\xi_l}\sigma_{\xi'_l}} \exp\left(\frac{-\xi_l^2}{2\sigma^2_{\xi_l}} + \frac{-\xi_l'^2}{2\sigma^2_{\xi'_l}}\right), \tag{16}$$

where $\sigma^2_{\xi_l}$ and $\sigma^2_{\xi'_l}$ are given in (13) and (15) respectively.

As can be seen in (16), $f(\xi_l, \xi'_l; l)$ is not a function of $l$. By Using (16) in (11), after some manipulations (see Appendix I) average number of zero-crossings over interval $(l_1, l_2)$ will be derived as

$$\overline{N}_z = \frac{l_2 - l_1}{\pi g} \sqrt{\frac{m(4) \int_{-\pi}^{\pi} \cos^2(\vartheta - \phi)\Omega(\vartheta) \mathrm{d}\vartheta}{m(0)}}. \tag{17}$$

On average, half of the $\overline{N}_z$ zero-crossings is dedicated to upwards and half to downwards over interval $(l_1, l_2)$. Thus, the average wavelength can be obtained as

$$\overline{\lambda} = \frac{l_2 - l_1}{\overline{N}_z/2} = 2\pi g \sqrt{\frac{m(0)}{m(4) \int_{-\pi}^{\pi} \cos^2(\vartheta - \phi)\Omega(\vartheta) \mathrm{d}\vartheta}}, \tag{18}$$

which can be interpreted as the average distance between two successive upward (downward) zero-crossings.

Substituting (18) in (10), we can approximate the envelope of normalized autocorrelation function in space domain. In Section V (i.e. the evaluation section), we will compare the

spatial autocorrelation function numerically calculated from (6) and the exponential envelope approximation expressed by (10) and (18). We will see the exponential approximation with respect to the average wave-length can properly describe the behavior of autocorrelation envelope.

## IV. Maximum Wave-height Blocking

In this section, we are going to investigate blocking probability of the link between a transmitter and a receiver located distance $L$ away from each other. We will use the same polar coordinate setup we defined in Section III. Hence, transmitter is located at the origin and polar coordination of receiver will be $(L, \phi)$, where $\phi$ is the angle from the positive side of x-axis.

Consider a homogeneous ocean WSN, where antenna heights of the transmitter and receiver are the same. According to [4], in such a network, an LoS link is blocked if there exists at least one ocean wave between the transmitter and receiver pair whose height exceeds a certain threshold ($H_{th}$). In other words, a link is blocked if the maximum wave-height between transmitter and receiver exceeds the threshold $H_{th}$, where the threshold $H_{th}$ is determined by the transmitter and receiver's antenna height. Hence, the blocking probability of the LoS link is equivalent to the probability that the maximum wave-height is larger than $H_{th}$.

Deriving the above probability is not easy since obtaining the global maximum of a curve is not a simple problem. It is even more complicated if the curve is random. To find the global maximum of a curve, one should first determine its local maxima and then compute the global maximum as the maximum of local maxima. Using this idea, we will first obtain the PDF of local maximum and then derive the PDF of global maximum based on the PDF of local maxima. Specifically, we will divide the distance between transmitter and receiver into semi-independent wave profiles, each of which has their own local maximum. Then, assuming identical and independent distribution (i.i.d.) for each profile's maximum, the global maximum PDF can be derived. Existence of one local maximum in each wave profile and these local maxima are independent are two of the approximations we made in order to compute the global maximum PDF. These approximations are necessary since finding the exact PDF of maximum of random variables is generally not soluble. In Section V, we will compare the statistics of approximated maximum wave-height with simulation results, which will show this approximation does not introduce significant errors.

In the remainder of this section, we are going to first drive PDF of the local maximum height of ocean surface displacement in Section IV-A and then derive the global maximum PDF in Section IV-B.

### A. Local Maximum of Wave-height

In this section, we are going to derive PDF of the local maximum wave-height in ocean. Local maxima of ocean surface displacement occur in the points at which the first derivative of curve is zero while the second derivative is negative. As can be seen in Fig. 1, local maximum is not necessarily a positive value. Consider the spatial surface displacement expression in polar coordinate system in (9). Fixing the polar angle $\phi$, in Section III, we defined $\xi(l)$ and $\xi'(l)$ as the ocean surface random curve and its derivative with respect to distance $l$, respectively. $\xi_l$ and $\xi'_l$ denoted spatial samples of $\xi(l)$ and $\xi'(l)$ at a certain $l$. Similarly, now let us define $\xi''(l)$ as the second order derivative of $\xi(l)$ with respect to $l$, and $\xi''_l$ as the sample of $\xi''(l)$ at a certain $l$. Since $\xi(l)$ is a WSS zero-mean Gaussian process, $\xi''(l)$ will be a WSS zero-mean Gaussian process and moreover, $\xi(l)$, $\xi'(l)$ and $\xi(l)''$ will be jointly WSS Gaussian processes [17]. Therefore $\xi_l$, $\xi'_l$, and $\xi''_l$ are jointly zero-mean Gaussian random variables that can be described by a multivariate normal distribution function $f(\xi_l, \xi'_l, \xi''_l)$ [17]. In [20], it is shown that the PDF of local maxima $\tilde{f}_{\max}(\xi_m)$ for the random curve $\xi(l)$ can be obtained as

$$\tilde{f}_{\max}(\xi_m) = \frac{\int_{-\infty}^{0} |\xi''_l| f(\xi_m, 0, \xi''_l) \mathrm{d}\xi''_l}{\int_{-\infty}^{\infty}\int_{-\infty}^{0} |\xi''_l| f(\xi, 0, \xi''_l) \mathrm{d}\xi''_l \mathrm{d}\xi}. \quad (19)$$

Since $\xi_l$, $\xi'_l$, and $\xi''_l$ are jointly zero-mean Gaussian random variables, $f(\xi_l, \xi'_l, \xi''_l)$ has the general form of

$$f(\xi_l, \xi'_l, \xi''_l) = \frac{1}{(2\pi)^{\frac{3}{2}} |\Sigma|^{\frac{1}{2}}} \exp\left(-\frac{1}{2} \underline{\xi}^T \Sigma^{-1} \underline{\xi}\right), \quad (20)$$

where $\underline{\xi} = [\xi_l, \xi'_l, \xi''_l]^T$, and $\Sigma = \mathbb{E}\{\underline{\xi}\, \underline{\xi}^T\}$ is the covariance matrix. $T$ denotes transpose and $|.|$ denotes the absolute determinant. $\Sigma$ is a $3 \times 3$ Hermitian matrix with elements corresponding to variances and covariances.

In order to obtain $\Sigma$'s elements, we should obtain auto/cross-correlation functions first. In III-B, we obtained autocorrelation functions of $\xi(l)$ and $\xi'(l)$ in (6) and (14) respectively, which leaded to find variances $\sigma^2_{\xi_l}$ in (13) and $\sigma^2_{\xi'_l}$ in (15) . As it has been mentioned, having i.i.d. set of harmonics' phases $\underline{\theta}$ uniformly distributed over $[-\pi, \pi)$ is the sufficient condition for $\xi(l)$ and $\xi'(l)$ to be uncorrelated. We will go through the same procedure for finding statistics of $\xi''_l$ as well. Based on probability theory about WSS stochastic process [17], the autocorrelation function of $\xi''(l)$ for a constant $\phi$, denoted as $R_{\xi''}(l, \phi)$, can be computed as:

$$R_{\xi''}(l, \phi) = \frac{\partial^4}{\partial l^4} R_{\xi}(l, \phi). \quad (21)$$

Considering (6) and (12), variance of $\xi''_l$ (denoted as $\sigma^2_{\xi''_l}$) can be obtain by substituting $l = 0$ in (21) which yields

$$\begin{aligned}\sigma^2_{\xi''_l} &= \int_{\omega=0}^{\infty}\int_{\vartheta=-\pi}^{\pi} \frac{\omega^8}{g^4} S(\omega) \cos^4(\vartheta - \phi) \Omega(\vartheta) \mathrm{d}\omega \mathrm{d}\vartheta \\ &= \frac{m(8)}{g^4} \int_{-\pi}^{\pi} \cos^4(\vartheta - \phi) \Omega(\vartheta) \mathrm{d}\vartheta.\end{aligned}$$

Similar to what we had for $\xi_l$ and $\xi'_l$, i.i.d. uniform phase assumption in harmonic waves makes $\xi'(l)$ and $\xi''(l)$ uncorrelated, which implies that $\xi'_l$ and $\xi''_l$ have zero correlation. However, $\xi_l$ and $\xi''_l$ are correlated. It can be shown that for

two jointly WSS stochastic processes $\xi(l)$ and $\xi''(l)$, the cross-correlation function $R_{\xi\xi''}(l,\phi)$ can be obtained as [17]

$$R_{\xi\xi''}(l,\phi) = \frac{\partial^2}{\partial l^2} R_{\xi}(l,\phi), \tag{22}$$

where $\phi$ is a constant phase. Covariance of $\xi_l$ and $\xi_l''$ will be obtain by choosing $l=0$ in (22) which will be equal to $-\sigma^2_{\xi_l'}$. Having all second order statistics of $\xi_l$, $\xi_l'$, and $\xi_l''$, covariance matrix $\Sigma$ will be given as

$$\Sigma = \begin{bmatrix} \sigma^2_{\xi_l} & 0 & -\sigma^2_{\xi_l'} \\ 0 & \sigma^2_{\xi_l'} & 0 \\ -\sigma^2_{\xi_l'} & 0 & \sigma^2_{\xi_l''} \end{bmatrix}. \tag{23}$$

By substituting (23) in (20), after some manipulations (see Appendix II.A), (19) will give the PDF of local maximum as

$$\begin{aligned} \tilde{f}_{\max}(\xi_m) = {} & \frac{\epsilon}{\sqrt{2\pi m(0)}} \exp\left(-\frac{1}{2\epsilon^2}\frac{\xi_m^2}{m(0)}\right) \\ & + \sqrt{1-\epsilon^2}\,\frac{\xi_m}{m(0)} \exp\left(-\frac{1}{2}\frac{\xi_m^2}{m(0)}\right) \\ & \times \Phi\left(\frac{\sqrt{1-\epsilon^2}}{\epsilon}\frac{\xi_m}{\sqrt{m(0)}}\right), \quad -\infty < \xi_m < \infty \end{aligned} \tag{24}$$

where $\epsilon = 1 - \sigma^4_{\xi_l'}/(\sigma^2_{\xi_l}\sigma^2_{\xi_l''})$, and $\Phi(.)$ denotes the Cumulative Distribution Function (CDF) of the standard normal distribution, i.e., $\Phi(x) = \frac{1}{\sqrt{2\pi}}\int_{-\infty}^{x} \exp\left(-\alpha^2/2\right) \mathrm{d}\alpha$. Using Cauchy-Schwarz inequality [17], it can be shown $0 \le \epsilon < 1$. CDF of the local maximum is derived as $\tilde{F}_{\max}(\xi_m) = \int_{-\infty}^{\xi_m} \tilde{f}_{\max}(\alpha)\mathrm{d}\alpha$, which after some manipulations (See Appendix II.B) yields

$$\begin{aligned} \tilde{F}_{\max}(\xi_m) = {} & \Phi\left(\frac{\xi_m}{\epsilon\sqrt{m(0)}}\right) \\ & - \sqrt{1-\epsilon^2}\exp\left(-\frac{\xi_m^2}{2m(0)}\right)\Phi\left(\frac{\sqrt{1-\epsilon^2}}{\epsilon}\frac{\xi_m}{\sqrt{m(0)}}\right). \end{aligned} \tag{25}$$

In the next section, we will use the obtained PDF and CDF of local maximum of ocean displacement curve for deriving the PDF of global maximum wave-height between transmitter and receiver. Then, we can use the global maximum PDF for calculating the link blocking probability.

### *B. Global Maximum of Wave-height*

In this section, we are going to derive the PDF of global maximum wave-height between transmitter and receiver, and use that for calculating the probability of a link to be blocked. In a random curve, global maximum can be obtained by finding the maximum of all local maxima. In general, the local maximum heights may not be independent, and finding the maximum among dependent random variables is generally mathematically insoluble. To resolve this challenge, we will divide the waves between the transmitter and receiver into semi-independent profiles. Assuming each profile has only one local maximum whose distribution is described by (24) and (25), we can obtain the approximated PDF of global maximum wave-height between a pair of transmitter and receiver.

As it has been mentioned before, $\xi(l)$ is a WSS zero-mean Gaussian process each of its samples on $l$ is a zero-mean Gaussian random variable. For this case, zero correlation is equivalent to independence of Gaussian samples. Considering the spatial autocorrelation approximation of (10), zero correlation will not happen unless $l$ tends to infinity. Therefore, similar to approaches usually used in wireless communication context [21], we define coherence distance $l_c$ as the distance within which waves behave statistically similar. In other word, $l_c$ corresponds to the distance inside which normalized correlation is close to 1. Therefore, those ocean waves whose distance from each other is farther than $l_c$ are weakly correlated and we consider them semi-independent. In this paper, we choose the concept of 3-dB decay for defining the coherence distance and in Section V, we will show global maximum statistics can be very accurately described using this definition. Specifically using the exponential approximation of normalized autocorrelation envelope in (10), 3-dB decay occurs when the envelope reaches to $\sqrt{2}/2$ of its maximum. Note that $20\log_{10}(\sqrt{2}/2) = -3$dB. Therefore, the coherence distance can be obtained as

$$l_c = -\log_e(\frac{\sqrt{2}}{2})\overline{\lambda} \approx 0.3466\overline{\lambda}, \tag{26}$$

where $\log_e(.)$ is natural logarithm and $\overline{\lambda}$ is the average wavelength obtained from (18).

Using the concept of coherence distance, we divide waves between the transmitter and receiver into $N = L/l_c$ semi-independent profiles, assuming only one local maximum is located in each profile and these local maxima of the semi-independent profiles are independent of each other. Let $\Xi_{\max}$ denotes the global maximum within the distance $L$. For $N$ independent random variables corresponding to local maxima, probability theory [17] says that PDF of $\Xi_{\max}$ can be computed as:

$$f_{\max}(\xi_m) = N\tilde{f}_{\max}(\xi_m)\tilde{F}_{\max}(\xi_m)^{N-1}, \tag{27}$$

where $\tilde{f}_{\max}(\xi_m)$ and $\tilde{F}_{\max}(\xi_m)$ are obtained in (24) and (25) respectively. For global maximum CDF we have

$$F_{\max}(\xi_m) = \Pr\{\Xi_{\max} \le \xi_m\} = \tilde{F}_{\max}(\xi_m)^N. \tag{28}$$

From now on, when we use maximum wave-height, we refer to global maximum of wave-height unless we mention local maximum explicitly. As we discussed before, a link is blocked if the maximum wave-height exceeds a certain threshold $H_{th}$. Using (28), we have

$$P_b = \Pr\{\Xi_{\max} > H_{th}\} = 1 - F_{\max}(H_{th}),$$

where $P_b$ denotes probability of blocking.

## V. Evaluation

In this section, we are going to evaluate our mathematical analysis results regarding LoS link blocking caused by ocean

waves. First, we demonstrate our simulation setup in Subsection V-A. Then we compare the exponential approximation of autocorrelation envelope we obtained in (10) with exact numerical results of (6) in Subsection V-B. Subsection V-C is dedicated for validating the approximations we made for obtaining the maximum wave-height and investigating the effect of wind speed in our analytical results. Finally in Subsection V-D we investigate the blocking probability of LoS link for different wind speeds.

### A. Simulation Setup

In our simulations, we chose the general model of wave spectrum proposed by oceanographers which has the form of [11], [15]

$$S(\omega) = A\omega^{-p}\exp(-B\omega^{-q}), \tag{29}$$

where $A$, $B$, $p$ and $q$ are constants that may differ between different wave models. In our simulation evaluation, we used Neumann spectrum, which is a well-known wave spectra widely used for theoretical analysis of wind generated waves. This wave spectrum sets $A = 3.05\text{m}^2/\text{s}^5 \times \frac{\pi}{2}$, $B = 2g^2/U_w^2$, $p = 6$, and $q = 2$ in (29) [22]. $U_w$ denotes the *surface wind speed* in ocean. For $S(\omega)$ of form (29), it can be shown that the $r$th moment can be expressed as [11]

$$m(r) = \frac{AB^{(r-p+1)/q}}{q}\Gamma\left(\frac{p-r-1}{q}\right), \tag{30}$$

where $\Gamma(.)$ is the gamma function defined as $\Gamma(x) = \int_0^\infty \alpha^{x-1}e^{-\alpha}\text{d}\alpha$.

For directional distribution, we chose the general cosine-power model widely used for analytical purposes which has the form of [14]

$$\Omega(\vartheta) = \frac{\Gamma(s+1)}{2\sqrt{\pi}\Gamma(s+\frac{1}{2})}\cos^{2s}\left(\frac{\vartheta}{2}\right)$$

where $s$ is a parameter related to the angular frequency which is out of the context of this paper to discuss about. One can find more details about this model in [14] and references therein. We set $s = 2$ in our simulations.

As it was discussed in Section IV, we used a polar coordinate system whose x-axis is set to the downwind and y-axis is crosswind. In this system, transmitter is located at the origin and receiver has the coordination of $(L, \phi)$. We set $\phi$ equal to $\pi/4$ in our simulations. Our simulation is done in MATLAB wherein we created a script file to generate instantiations of ocean waves using the polar model of (9).

### B. Accuracy of the Envelop Approximation of Autocorrelation Function

In our first set of simulation, we set wind speed $U_w$ equal to 5m/s. The purpose of this simulation set is to validate the envelope of the spatial autocorrelation function of ocean wave that we have derived in (10).

Fig. 2 compares the exponential envelope approximation of autocorrelation function in (10), which is the red line, with the actual value of the autocorrelation functions under different spatial distance. Two lines of the autocorrelation functions are shown. The green line is obtained from simulated ocean wave instantiations and the black link is numerically computed from (6).

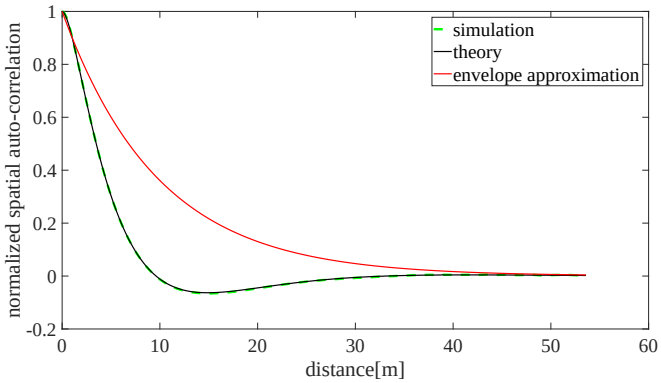


Fig. 2: Normalized spatial autocorrelation function and its envelope approximation

It can be seen that this envelope approximation is not tight for short distances. However, it provides a conservative and easily computable estimation of the coherence distance $l_c$. Using this simple expression, we can obtained the number of semi-independent wave profiles and consequently maximum wave-height PDF and CDF, which our following simulations show to match accurately with the simulation results.

### C. Accuracy of the maximum wave-height approximation

As it has been mentioned in Section IV, our link blocking probability is estimated based on an approximated estimation of maximum wave-height distribution. For validating the PDF and CDF of maximum wave-height and having a sense about its behavior when other parameters change, in our second set of simulations, we investigated the expected value of maximum wave-height in two different scenarios.

The first scenario examines the average value of maximum wave-height when the distance between transmitter and receiver changes. Fig. 3 depicts the average value of maximum wave-height when $L$ varies from 35m to 2.7km while $U_w = 3$, 4, 5 and 6 m/s. As can be seen, the theoretical approximated results match perfectly with the acutal maximum wave-height obtained in ocean wave simulations. It can be observed that the average maximum wave-height gets larger as the distance between transmitter and receiver increases. This is because the farther receiver is located from the transmitter, the more probable occurrence of larger waves in between. Another important observation is that by increasing the distance between transmitter and receiver, average maximum wave-height tends to a saturated value since the energy of waves is constant.

In the second scenario, we set the distance between transmitter and receiver to $L = 400$m and swept the wind speed from $U_w = 1$m/s to $U_w = 20$m/s and obtained average maximum wave-height accordingly. Fig. 4 compares the theoretical results with simulation, which match very well. As can be seen, increasing the wind speed is equivalent to have more power in ocean waves, which results in larger average

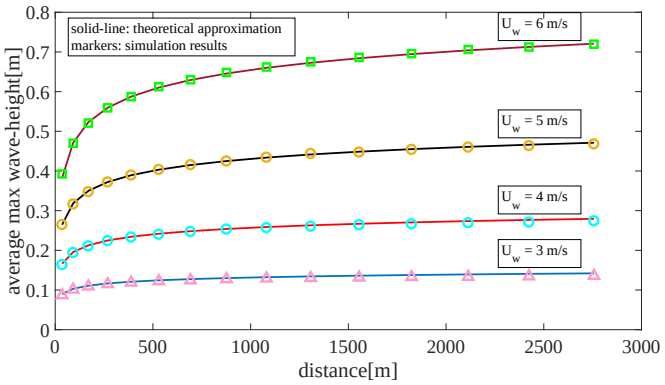


Fig. 3: Average maximum wave-height for different distances between transmitter and receiver

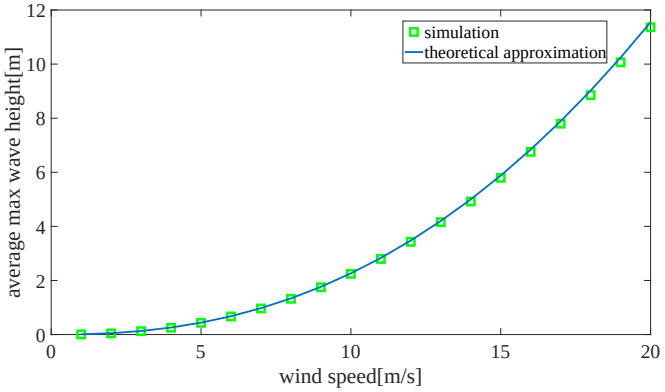


Fig. 4: Average maximum wave-height for different wind speeds

maximum wave-heights. In order to validate our simulation and theoretical approximation with reality, we compared our results with significant wave-height[1] measurements in [22, Fig. 8.4-2] . In these measurements, it has been shown that by increasing the wind speed from $U_w = 0$m/s to $U_w = 20$m/s, significant wave-height starts from 0m and exponentially grows to 12.5m. Therefore, the values of average maximum wave-height and its semi-exponential behavior we obtained in Fig. 4 grows in the same scale trend as real-world measurement and can be applied for real ocean waves.

### *D. Accuracy of link blocking probability*

After validating the PDF of maximum wave-height, for the final step, we are going to evaluate our model of the LoS link blocking probability. Sweeping $H_{th}$, Fig. 5 depicts plots of $P_b$ for $U_w = 3$, 4, 5, and 6 m/s. It can be seen that simulation results have fairly accurate matching with our theoretical approximation of maximum wave-height blocking. As it was shown in Fig. 4, by increasing the wind speed, average maximum wave-height will grow. Thus, for faster wind speeds, it is more probable to have higher waves, which results in higher probability of blocking and shifting $P_b$ to the right.

[1]In oceanography, significant wave-height is defined as the mean of the highest one-third of waves [22]

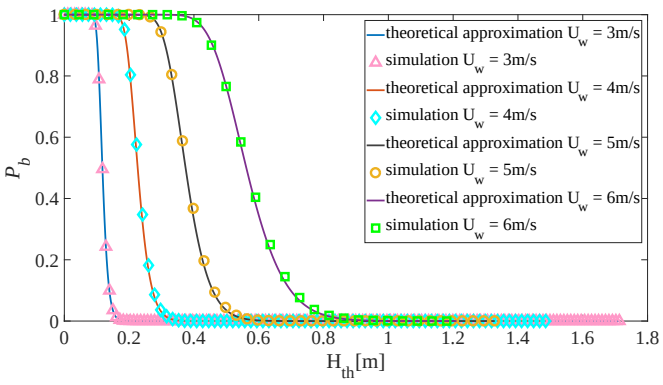


Fig. 5: Link block probability in different wind speeds

## VI. Conclusion

Link stability is an important network design consideration for ocean surface WSN. In this paper, we present a thorough analysis on the link stability for ocean surface communications based on realistic ocean surface model and derive a highly accurate closed-form expression for the LoS link's blocking probability. The accuracy of the expression is validated through extensive simulation under different ocean weather conditions. Our future work will focus on how to leverage this link stability model in the planning and design of ocean WSN.

## Appendix I
## Average Number of Zero-crossings

In this section, we are going to derive the average number of zero-crossings in (17). As it has been mentioned in Section III-B, the joint PDF of $f(\xi_l, \xi_l'; l)$ in (16) is not a function of $l$. Hence, substituting $f(0, \xi_l'; l)$ in (11) we have

$$\begin{aligned}\overline{N}_z &= (l_2 - l_1)\int_{\xi_l'=-\infty}^{\infty} \frac{|\xi_l'|}{2\pi\sigma_{\xi_l}\sigma_{\xi_l'}} \exp(\frac{-\xi_l'^2}{2\sigma_{\xi_l'}^2})\mathrm{d}\xi_l' \\ &= \frac{l_2 - l_1}{\pi\sigma_{\xi_l}\sigma_{\xi_l'}}\int_0^{\infty} \xi_l' \exp(\frac{-\xi_l'^2}{2\sigma_{\xi_l'}^2})\mathrm{d}\xi_l' = (l_2 - l_1)\frac{\sigma_{\xi_l'}}{\sigma_{\xi_l}},\end{aligned}$$

which yields (17) by substituting $\sigma_{\xi_l}$ and $\sigma_{\xi_l'}$ with (13) and (15) respectively.

## Appendix II
## PDF and CDF of Local Maximum of Ocean Surface Displacement

### *A. PDF*

In this subsection, we are going to derive the PDF of local maximum of wave-height in (24). For the first step, we should obtain the expression corresponding to the multivariate normal

distribution of (20). Substituting the covariance matrix of (23) in (20) we have

$$f(\xi_l,0,\xi_l'') = \frac{1}{(2\pi)^{3/2}\sigma_{\xi_l'}\sqrt{\Delta}} \exp\left(-\frac{\sigma_{\xi_l''}^2\xi_l^2 + 2\sigma_{\xi_l'}^2\xi_l\xi_l'' + \sigma_{\xi_l}^2\xi_l''^2}{2\Delta}\right) \quad (31)$$

where $\Delta = \sigma_{\xi_l}^2\sigma_{\xi_l''}^2 - \sigma_{\xi_l'}^4$. Having $f(\xi_l,0,\xi_l'')$, we are be able to use (19) for obtaining $\tilde{f}_{\max}(\xi_m)$. Substituting (31) in (19), the numerator becomes

$$\int_{-\infty}^{0} |\xi_l''| f(\xi_m,0,\xi_l'')\mathrm{d}\xi_l'' = \frac{\sigma_{\xi_l''}}{2\pi\sigma_{\xi_l'}}\left[\frac{\epsilon}{\sqrt{2\pi m(0)}}\exp\left(-\frac{1}{2\epsilon^2}\frac{\xi_m^2}{m(0)}\right) + \sqrt{1-\epsilon^2}\frac{\xi_m}{m(0)}\exp\left(-\frac{1}{2}\frac{\xi_m^2}{m(0)}\right) \times\Phi\left(\frac{\sqrt{1-\epsilon^2}}{\epsilon}\frac{\xi_m}{\sqrt{m(0)}}\right)\right] \quad (32)$$

and denumerator becomes

$$\int_{-\infty}^{\infty}\int_{-\infty}^{0} |\xi_l''| f(\xi,0,\xi_l'')\mathrm{d}\xi_l''\mathrm{d}\xi = 2\pi\frac{\sigma_{\xi_l'}}{\sigma_{\xi_l''}}. \quad (33)$$

Finally, by substituting (32) and (33) in (19), $\tilde{f}_{\max}(\xi_m)$ will be given in form of (24).

### B. CDF

After deriving the PDF of local maximum in (24), CDF can be obtained as

$$\begin{aligned}\tilde{F}_{\max}(\xi_m) &= \int_{-\infty}^{\xi_m}\tilde{f}_{\max}(\alpha)\mathrm{d}\alpha \\ &= \int_{-\infty}^{\xi_m}\frac{\epsilon}{\sqrt{2\pi m(0)}}\exp\left(-\frac{1}{2\epsilon^2}\frac{\alpha^2}{m(0)}\right)\mathrm{d}\alpha \equiv I_1 \\ &\quad + \int_{-\infty}^{\xi_m}\sqrt{1-\epsilon^2}\frac{\alpha}{m(0)}\exp\left(-\frac{1}{2}\frac{\alpha^2}{m(0)}\right) \\ &\quad \times\Phi\left(\frac{\sqrt{1-\epsilon^2}}{\epsilon}\frac{\alpha}{\sqrt{m(0)}}\right)\mathrm{d}\alpha \equiv I_2. \quad (34)\end{aligned}$$

In (34), $I_1$ will be computed as $\epsilon^2\Phi\left(\frac{\xi_m}{\epsilon\sqrt{m(0)}}\right)$. For calculating $I_2$, we can use the integration by part rule. Specifically, by choosing $\mathrm{d}u = \frac{\alpha}{m(0)}\exp\left(-\frac{\alpha^2}{2m(0)}\right)\mathrm{d}\alpha$ and $v = \Phi\left(\frac{\sqrt{1-\epsilon^2}}{\epsilon}\frac{\alpha}{\sqrt{m(0)}}\right)$, we have

$$\begin{aligned}I_2 &= -\sqrt{1-\epsilon^2}\exp\left(-\frac{\xi_m^2}{2m(0)}\right)\Phi\left(\frac{\sqrt{1-\epsilon^2}}{\epsilon}\frac{\xi_m}{\sqrt{m(0)}}\right) \\ &\quad + \sqrt{1-\epsilon^2}\int_{-\infty}^{\xi_m}\exp\left(-\frac{\alpha^2}{2m(0)}\right)\times\frac{1}{\sqrt{2\pi}}\frac{\sqrt{1-\epsilon^2}}{\epsilon\sqrt{m(0)}} \\ &\quad \times\exp\left(-\frac{\alpha^2}{2}\frac{1-\epsilon^2}{\epsilon^2 m(0)}\right)\mathrm{d}\alpha. \quad (35)\end{aligned}$$

After some manipulations, integral of (35) will be simplified as $(1-\epsilon^2)\Phi\left(\frac{\xi_m}{\epsilon\sqrt{m(0)}}\right)$. Hence, the CDF of (25) will be given by $\tilde{F}_{\max}(\xi_m) = I_1 + I_2$.

## REFERENCES


[1] G. Xu, W. Shen, and X. Wang, "Applications of wireless sensor networks in marine environment monitoring: A survey," *Sensors*, vol. 14, no. 9, pp. 16 932–16 954, 2014.

[2] J. Tateson, C. Roadknight, A. Gonzalez, T. Khan, S. Fitz, I. Henning, N. Boyd, C. Vincent, and I. Marshall, "Real world issues in deploying a wireless sensor network for oceanography," *REALWSN 2005*, 2005.

[3] M. Jiang, Z. Guo, F. Hong, Y. Ma, and H. Luo, "Oceansense: A practical wireless sensor network on the surface of the sea," in *Pervasive Computing and Communications, 2009. PerCom 2009. IEEE International Conference on*. IEEE, 2009, pp. 1–5.

[4] D. C. Steere, A. Baptista, D. McNamee, C. Pu, and J. Walpole, "Research challenges in environmental observation and forecasting systems," in *Proceedings of the 6th annual international conference on Mobile computing and networking*. ACM, 2000, pp. 292–299.

[5] S. M. Glenn, T. D. Dickey, B. Parker, and W. Boicourt, "Long-term real-time coastal ocean observation networks," *Oceanography*, vol. 13, no. 1, pp. 24–34, 2000.

[6] L. Yee Hui, F. Dong, and Y. S. Meng, "Near sea-surface mobile radiowave propagation at 5 ghz: measurements and modeling," *Radio-engineering*, vol. 23, no. 3, p. 825, 2014.

[7] T. Yapicioglu and S. Oktug, "Effect of wave height to connectivity and coverage in sea surface wireless sensor networks," in *Computer and Information Sciences, 2009. ISCIS 2009. 24th International Symposium on*. IEEE, 2009, pp. 328–333.

[8] J. G. de Boer, "On the correlation functions in time and space of wind-generated ocean waves," SACLANT ASW RESEARCH CENTRE LA SPEZIA (ITALY), Tech. Rep., 1969.

[9] G. Latta and J. Bailie, "On the autocorrelation functions of wind generated ocean waves," *Zeitschrift für angewandte Mathematik und Physik ZAMP*, vol. 19, no. 4, pp. 575–586, 1968.

[10] C. Bourlier, J. Saillard, and G. Berginc, "Intrinsic infrared radiation of the sea surface," *Journal of electromagnetic waves and applications*, vol. 14, no. 4, pp. 551–561, 2000.

[11] S. R. Massel, *Ocean surface waves: their physics and prediction*. World scientific, 2013, vol. 36.

[12] L. H. Holthuijsen, *Waves in oceanic and coastal waters*. Cambridge university press, 2010.

[13] J. Tessendorf *et al.*, "Simulating ocean water," *Simulating nature: realistic and interactive techniques. SIGGRAPH*, vol. 1, no. 2, p. 5, 2001.

[14] S. F. Barstow, J.-R. Bidlot, S. Caires, M. A. Donelan, W. M. Drennan, H. Dupuis, H. C. Graber, J. J. Green, O. Gronlie, C. Guérin *et al.*, "Measuring and analysing the directional spectrum of ocean waves," 2005.

[15] S. K. Chakrabarti, *Hydrodynamics of offshore structures*. WIT press, 1987.

[16] P. Rudnick, "Correlograms for pacific ocean waves," UNIVERSITY OF CALIFORNIA MARINE PHYSICAL LABORATORY San Diego United States, Tech. Rep., 1951.

[17] A. Papoulis and S. U. Pillai, *Probability, random variables, and stochastic processes*. Tata McGraw-Hill Education, 2002.

[18] S. O. Rice, "Mathematical analysis of random noise," *The Bell System Technical Journal*, vol. 24, no. 1, pp. 46–156, 1945.
[19] M. K. Ochi, *Ocean waves: the stochastic approach*. Cambridge University Press, 2005, vol. 6.
[20] D. E. Cartwright and M. S. Longuet-Higgins, "The statistical distribution of the maxima of a random function," *Proc. R. Soc. Lond. A*, vol. 237, no. 1209, pp. 212–232, 1956.
[21] A. Goldsmith, *Wireless communications*. Cambridge university press, 2005.
[22] B. Kinsman, *Wind waves: their generation and propagation on the ocean surface*. Courier Corporation, 1984.